

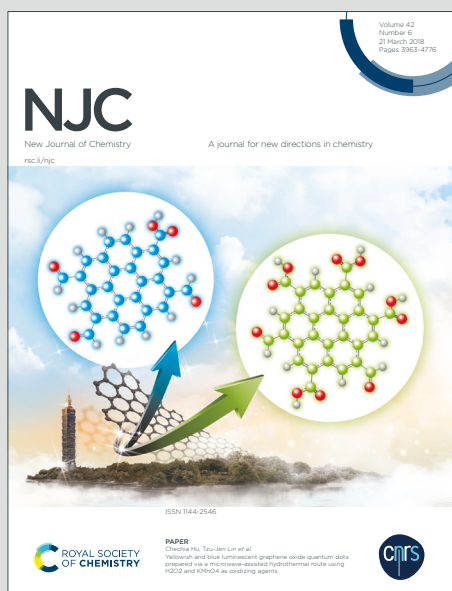
NJC

New Journal of Chemistry

Accepted Manuscript

A journal for new directions in chemistry

This article can be cited before page numbers have been issued, to do this please use: J. Yang, F. Huo, K. Ma, Y. yue and C. Yin, *New J. Chem.*, 2020, DOI: 10.1039/D0NJ04484A.



This is an Accepted Manuscript, which has been through the Royal Society of Chemistry peer review process and has been accepted for publication.

Accepted Manuscripts are published online shortly after acceptance, before technical editing, formatting and proof reading. Using this free service, authors can make their results available to the community, in citable form, before we publish the edited article. We will replace this Accepted Manuscript with the edited and formatted Advance Article as soon as it is available.

You can find more information about Accepted Manuscripts in the [Information for Authors](#).

Please note that technical editing may introduce minor changes to the text and/or graphics, which may alter content. The journal's standard [Terms & Conditions](#) and the [Ethical guidelines](#) still apply. In no event shall the Royal Society of Chemistry be held responsible for any errors or omissions in this Accepted Manuscript or any consequences arising from the use of any information it contains.

Water soluble ratiometric fluorescent probe to mitochondrial targeted SO₂ based on conjugated biquinolines

Received 00th January 20xx,
Accepted 00th January 20xx

DOI: 10.1039/x0xx00000x

Jialu Yang^a, Caixia Yin, ^{a,*} Kaiqing Ma, ^aYongkang Yue, ^aFangjun Huo^{b,*}

Despite the unprecedented development of SO₂ fluorescent probes in the past five years, the water-solubility of probes is still an important factor related to their practical application. In previous work, we have studied SO₂ detection by coupling quinoline and coumarin. Although the water solubility of probe was improved, the detection in the 100% aqueous medium was not fully achieved. Therefore, based on the previous system, we conjugated two quinolines to realize a 100% water-soluble sulfur dioxide fluorescent probe. The **Probe** showed a large Stokes-shift (170 nm). Besides, the **Probe** could respond to SO₂ within 1.5 min with high selectively and sensitively (LOD = 0.29 μM). In addition, fluorescence co-localization studies suggested that the **Probe** could be used for monitoring SO₂ in the mitochondria of HeLa cells and living mice. It is believed that such an excellent probe will have a wide application prospect in the future.

1. Introduction

For a long time, environmental and health issues have received great attention. Sulfur dioxide (SO₂) is used as a global atmospheric pollutant frequently, but it is widely used as food additive due to its excellent antioxidant properties, corrosion protection, and color retention.¹ Therefore, SO₂ has great effect on human health. However, articles show that the emission of SO₂ is not only aggravating the air pollution, but also related to the occurrence of many diseases.²⁻⁵ Endogenous SO₂ mainly exists in the mitochondria of cells. It is formed by the oxidation of H₂S⁶⁻⁷ and some sulfur-containing amino acids.⁸⁻¹³ After being absorbed into the human body, it is first converted into its derivatives-sulfite and bisulfite in body fluids.¹⁴⁻¹⁵ These derivatives can not only damage the respiratory system, but also enter the blood in the form of ions and distribute to the whole body, causing a variety of organ damage. Therefore, it is necessary to track and detect SO₂ and its derivatives in the mitochondria of subcellular organelles.

As a powerful visual biological imaging method, fluorescent probe is widely used because of its strong designability, high spatial-temporal resolution and high sensitivity.¹⁶⁻²⁴ A lot of fluorescent probes are used to detect SO₂ derivatives in vitro and vivo in recent years. The detection mechanism includes:

nucleophilic addition of SO₂ to aldehyde group,²⁵⁻²⁶ decomposition of levulinic acid mediated by HSO₃,²⁷ Michael addition and coordination.²⁸⁻²⁹ However, these fluorescent probes have some defects, poor water solubility (Table 1) and are often interfered by other mercaptan competitive substances. In addition, the single emission type fluorescent probe has a single emission wavelength and the SO₂ in the sensor body will be interfered by other environmental factors.³⁰ In contrast, the ratio type fluorescence probe uses its fluorescence emission ratio at different wavelengths as the detection signal, which can be more accurate.³¹⁻³⁴

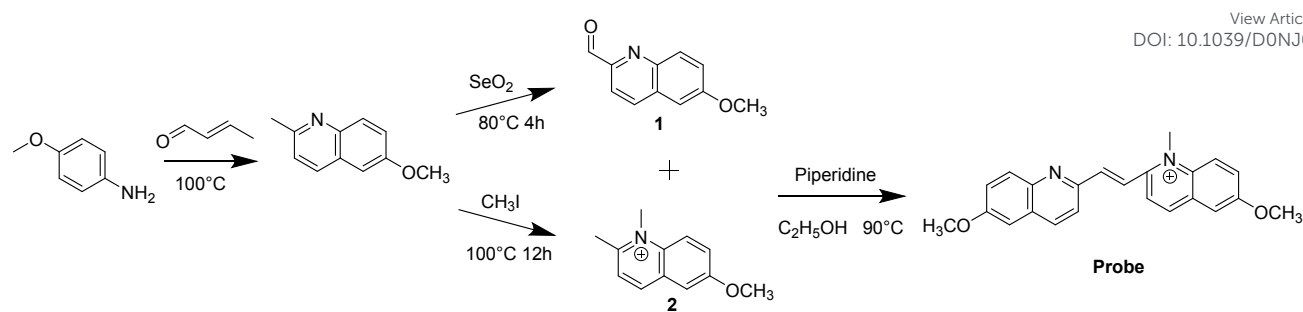
In our previous research, we designed a SO₂ fluorescent probe through the conjugation of quinoline and coumarin, which greatly improved the water solubility of the probe.³⁵ However, the detection system still required organic solvents to help dissolve. Based on this foundation, two quinolines were conjugated by double bonds to construct **Probe**.³⁶ Moreover, the common mitochondrial targeting probes usually show small Stokes shift and are affected by external factors. Compared to this, after the **Probe** reacted with NaHSO₃ in water, the **Probe** responded quickly and showed proportional fluorescence emission. In addition, the **Probe** showed a large Stokes shift (170 nm), which was more likely to avoid background fluorescence interference. In living cell imaging, **Probe** accumulated in mitochondria. In addition, **Probe** had been made use of imaging in mice successful.

^a Key Laboratory of Chemical Biology and Molecular Engineering of Ministry of Education, Institute of Molecular Science, Shanxi University, Taiyuan, 030006, China.

^b Research Institute of Applied Chemistry, Shanxi University, Taiyuan, 030006, China..

† Footnotes relating to the title and/or authors should appear here.

Electronic Supplementary Information (ESI) available: [details of any supplementary information available should be included here]. See DOI: 10.1039/x0xx00000x



Scheme 1. The synthetic route of the Probe.

2 Result and Discussion

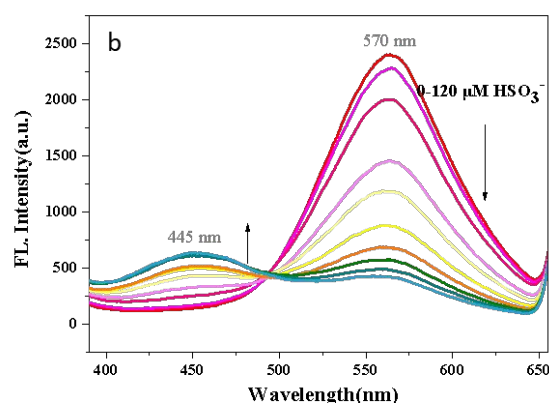
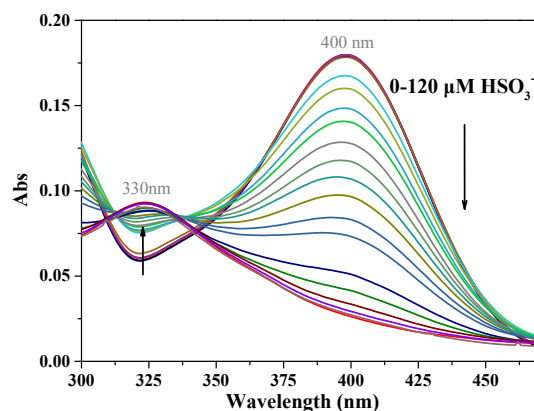
2.1. Characterization data of the Probe

Scheme 1 shows the **Probe** synthesis route. **Probe** was synthesized according to the literature.³⁷ The synthetic routes of other compounds are listed in the supporting information.

The **Probe** was characterized by NMR and HR-MS. ¹H NMR (600 MHz, DMSO-*d*₆) δ 9.00 (d, *J* = 8.8 Hz, 1H), 8.62 (d, *J* = 8.8 Hz, 1H), 8.56 (d, *J* = 10.3 Hz, 1H), 8.44 (d, *J* = 8.4 Hz, 1H), 8.31 (d, *J* = 15.8 Hz, 1H), 8.16 (dd, *J* = 21.2, 12.2 Hz, 2H), 8.02 (d, *J* = 9.1 Hz, 1H), 7.87 (d, *J* = 5.7 Hz, 2H), 7.51 – 7.45 (m, 2H), 4.61 (s, 3H), 4.02 (s, 3H), 3.95 (s, 3H). ¹³C NMR (151 MHz, DMSO-*d*₆) δ 159.44 (s), 158.83 (s), 153.31 (s), 151.20 (s), 144.80 (s), 144.22 (s), 143.72 (s), 136.18 (d, *J* = 42.4 Hz), 135.27 (s), 131.26 (s), 130.76 (s), 129.85 (s), 127.18 (s), 123.73 (s), 123.67 (s), 122.49 (s), 122.27 (s), 121.75 (s), 108.77 (s), 106.21 (s), 56.76 (d, *J* = 3.4 Hz), 56.18 (d, *J* = 4.0 Hz), 40.82 (d, *J* = 8.7 Hz). The HR-MS spectrum of **Probe**: calc. for C₂₃H₂₁N₂O₂⁺[M]⁺, 357.15975, found 357.15973.

2.2. Optical characteristics of the Probe

In the PBS test system, we evaluated the response of the **Probe** to SO₂ through ultraviolet spectrophotometer and fluorescence spectrophotometer. As shown in Figure 1a, after the continuous mixing of NaHSO₃, the strong absorption peak gradually decreased until the peak disappeared (400 nm). Meanwhile, a peak appeared at 330nm gradually. As for the fluorescence spectrum (Figure 1b), under the excitation of 330 nm, with the addition of 120 μM SO₂, the strong fluorescent emission of the **Probe** at 570 nm continued to decline and reached a saturation, and a emission peak arised at 445 nm, which proved that the new substance was produced in the reaction process. At the same time, we also conducted a spectral test on the stability of the **Probe** (Figure S5), which showed that the **Probe** had excellent photostability. In addition, the **Probe** showed a large Stokes shift of 170 nm (Figure 1c), effectively avoiding excitation backscattering effects.



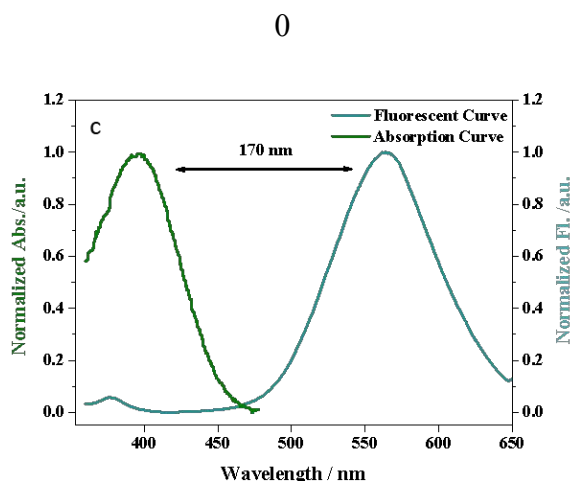


Figure 1 (a) In the PBS, the Ultraviolet spectrum of the **Probe** (10 μM) coexisted with different concentrations of NaHSO_3 (0-120 μM). pH = 7.4 (b) The fluorescence spectrum of the **Probe** (10 μM) coexisted with different concentrations of NaHSO_3 (0-120 μM) in PBS solution (pH = 7.4), $\lambda_{\text{ex}} = 330 \text{ nm}$, slit width: 5 nm / 10 nm. (c) The normalized absorption (green) and fluorescence (blue) spectra of **Probe**.

During the contact of the **Probe** with HSO_3^- , the reaction was rapidly and the reaction was almost completed in a short time (1.5 min). The fluorescence intensity was basically flat in the system where only **Probe** existed. This indicated that **Probe** had the ability to respond quickly to SO_2 , and had the potential to detect SO_2 in real time in living organisms.

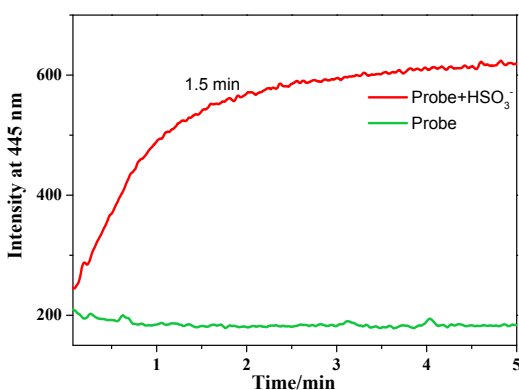


Figure 2 In PBS solution, the fluorescence intensity changes at 445 nm with time when excess NaHSO_3 (120 μM) coexisted with the **Probe** (10.0 μM). pH = 7.4, $\lambda_{\text{ex}} = 330 \text{ nm}$, slit width: 5 nm / 10 nm at room temperature.

2.3 Selectivity of the Probe

Whether it has a single excellent selectivity is very important for **Probe**, so we evaluated it by fluorescence spectroscopy. First, **Probe** interacted with other amino acids in PBS buffer, which can be compared with the HSO_3^- treated system. The fluorescence intensity emission ratio was significantly higher than the ratio after other amino acid treatments (Figure 3a). Similarly, under the same external additional conditions, **Probe** interacted with other anions. The ratio of fluorescence intensity was still much lower than the ratio with HSO_3^- action (Figure 3b). When HSO_3^- was added to other amino acids, it can be clearly seen that the ratios have increased by different amplitudes in the competition graph. (Figure S6-7) Therefore, from all these results, we can conclude that the **Probe** has outstanding selectivity for SO_2 .

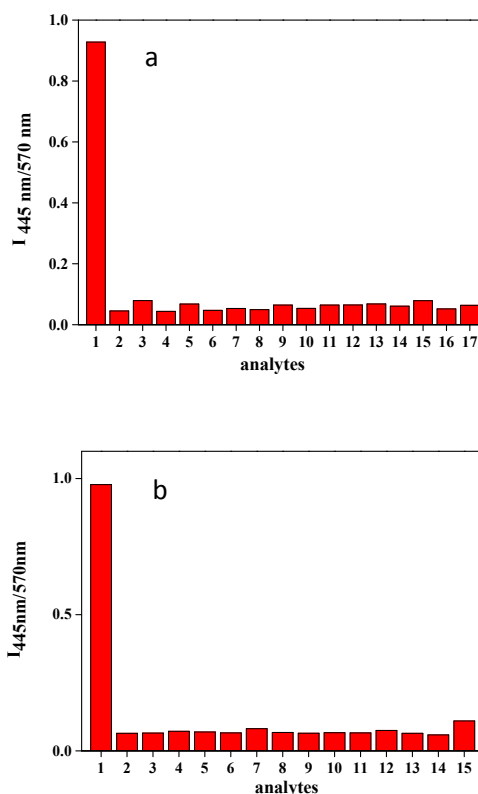


Figure 3. (a) In the existence of other amino acids each (5 mM), the ratio value of the **Probe** (10 μM) in PBS solution (pH=7.4), slit width: 5 nm/10 nm. 1. NaHSO_3 , 2. H_2S , 3. L-Threonine, 4. L-Methionine, 5. L-Proline, 6. L-Aspartic acid, 7. L-Valine, 8. trans-4-Hydroxy-L-proline, 9. L-Asparagine, 10. L-Glutamic acid, 11. L-phenylalanine, 12. L-Arginine, 13. L-Isoleucine, 14. Cys, 15. GSH, 16. Hcy, 17. L-Leucine. All data were obtained after waiting for 3 minutes. (b) In the existence of other anions each (5 mM), the fluorescence intensity of the **Probe** (10 μM) in PBS solution (pH=7.4), slit width: 5 nm/10 nm. 1. NaHSO_3 , 2. CH_3COO^- , 3. Cl^- , 4. CO_3^{2-} , 5. F^- , 6. H_2PO_4^- , 7. ClO^- , 8. HCO_3^- , 9. HPO_4^{2-} , 10. SO_4^{2-} , 11. Br^- , 12. NO_2^- , 13. SCN^- , 14. $\text{S}_2\text{O}_3^{2-}$, 15. H_2O_2 . All data were obtained after waiting for 3 minutes.

2.4 pH dependence and the detection limit of the Probe

We explored the physiological and environmental effects of coexistence of **Probe** and SO_2 under different pH conditions. It is obvious from the figure (Figure S8) that the fluorescence intensity ratio between pH 7-10 has a large increase. This is good for detecting SO_2 in a physiological environment. Furthermore, the detection limit is also an important content that cannot be ignored in evaluating probe functionality. After precise tests and calculations, on the basis of the definition of IUPAC ($\text{CDL} = 3 S_b/m$), the detection limit of the **Probe** was $0.29 \mu\text{M}$. It showed that in the PBS test solution, the **Probe** has a high sensitivity to HSO_3^- .

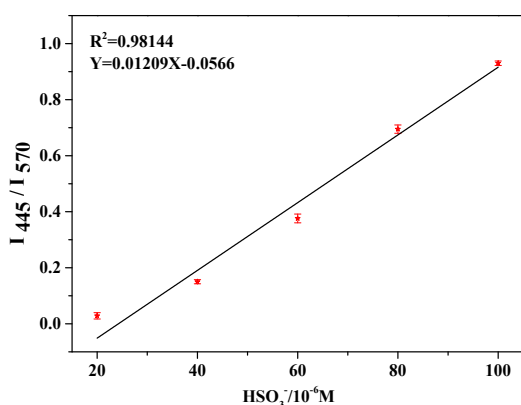


Figure 4. The relationship between fluorescence intensity and NaHSO_3 concentration was linear.

2.5 Detection mechanism

The design initially intended to form a conjugated system for two large quinoline rings. The **Probe** showed a certain fluorescence intensity at 570 nm under the excitation of 330 nm when the double bond was not added. After the addition of NaHSO_3 , the double bond addition and the large conjugated system were destroyed, showing the fluorescence of the quinoline ring at 445 nm. In Figure S4, we verified its mechanism. The product $[\text{C}_{23}\text{H}_{22}\text{N}_2\text{NaO}_5\text{S}^+]$ in high-resolution mass spectrometry should be $m/z: 461.11416$ and the product $m/z: 461.11359$ confirmed our assumption.

2.6 The cytotoxicity and live cell imaging.

After the spectral experiment, because of the excellent spectral properties of the **Probe**, we carried out further biological imaging experiments to prove that the **Probe** can detect small molecular sulfur in cells. First, we measured the cytotoxicity of the **Probe**. We incubated different concentrations of **Probe** for 5 h and 10 h in HeLa cells, and found that the survival percentage of HeLa cells was 91% (Figure S9). The excellent low toxicity of the **Probe** can pave the way for our next cell imaging experiment.

In the exogenous experiment of cell imaging, we incubated the **Probe** ($10 \mu\text{M}$) into HeLa cells at 37°C for 20 min. It was obvious

that the **Probe** exhibited strong fluorescence emission in the yellow channel and almost no light in the blue channel. After incubated $50 \mu\text{M}$ and $100 \mu\text{M}$ HSO_3^- into the cells, it can be seen from the Figure 5b-5c that with the increase of HSO_3^- , the fluorescence of yellow channel was gradually weakened and the fluorescence of blue channel was further enhanced. These results demonstrated that **Probe** can respond to exogenous SO_2 . After implemented the exogenous cell experiment, we detected the endogenous SO_2 . HeLa cells were cultured with **Probe** ($10 \mu\text{M}$) for 20 min, and cultured with $200 \mu\text{M}$ Cys [30]. After washed with PBS, we found that the fluorescence of the yellow channel was significantly decreased and that of the blue channel was enhanced compared with the **Probe** only. This also illustrated that the **Probe** can be a powerful testing means to detect endogenous SO_2 in living cells.

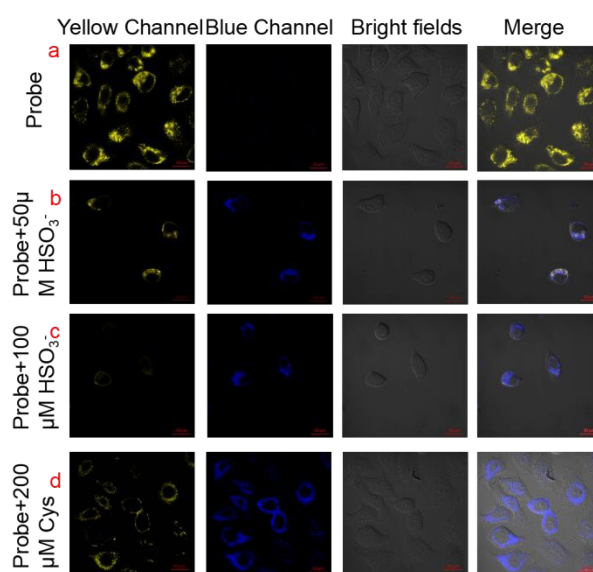


Figure 5 (a) The **Probe** ($10 \mu\text{M}$) and HeLa cells were co-cultured for 20 min for cell imaging; (b) incubation with NaHSO_3 ($50 \mu\text{M}$); (c) After pretreatment of the **Probe** ($10 \mu\text{M}$) with HeLa cells for 20 min, the cell images obtained after 20 min of incubation with NaHSO_3 ($100 \mu\text{M}$); (d) Cys ($200 \mu\text{M}$) was incubated for 15 min after the **Probe** ($10 \mu\text{M}$) incubated with HeLa cells for 20 min. Yellow channel, $\lambda_{\text{em}} = 540\text{-}600 \text{ nm}$, $\lambda_{\text{ex}} = 488 \text{ nm}$; Blue channel: $\lambda_{\text{em}} = 420\text{-}480 \text{ nm}$, $\lambda_{\text{ex}} = 405 \text{ nm}$. Scale bar: $20 \mu\text{m}$.

We further explored the function of the **Probe** targeting the subcellular organelle mitochondria. We incubated the **Probe** into HeLa cells for 20 min, and then added with mitochondrial dye-Mito Tracker Red (MTR) ($1 \mu\text{M}$) for 20 min after washing with PBS. It can be seen in the combined images that the mitochondrial dye and the **Probe** were well overlapped ($R=0.91$), indicated that the **Probe** can exist in the mitochondria after entering the cell. These results indicated that the **Probe** has a targeting function on mitochondria and can be used for cell imaging of SO_2 in

mitochondria.

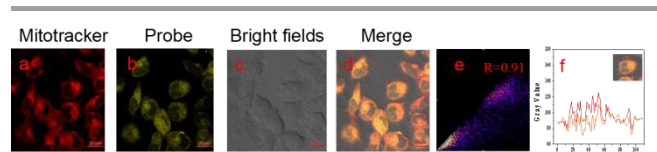


Figure 6 The co-localization image of the cells co-cultured with the **Probe** (10 μM) and Mitotracker red (1 μM). (a) Indicates the red channel (mitochondrial dye staining); (b) Indicates yellow channel (probe staining); (c) Indicates bright field; (d) Indicates merged images; (e) Correlation $R=0.91$. (f) Intensity profile of linear region of interest across the HeLa cell costained with Yellow channel of **Probe** and Mitotracker Red; Red channel, $\lambda_{\text{em}}=660\text{-}720\text{ nm}$, $\lambda_{\text{ex}}=633\text{ nm}$; Yellow channel: $\lambda_{\text{em}}=540\text{-}600\text{ nm}$, $\lambda_{\text{ex}}=488\text{ nm}$. Scale bar: 20 μm .

3.7 The imaging of Probe in mice

Then we studied the SO_2 imaging of **Probe** in mice. Before the injection of **Probe** and HSO_3^- , we photographed the blank mice and found that there was no fluorescence signal. After injected **Probe** into the abdominal cavity of mice, a strong fluorescent signal was observed. After intraperitoneal injection of HSO_3^- solution, photographs were taken at different times. It can be seen from the Figure 7c-7d that the fluorescence signal gradually weakened after 30 min. We added an experiment, only the probe was shot at different times when the probe was injected into the abdominal cavity of the mouse. From Figure 7e-7h, it can be clearly seen that within 120 min, the fluorescence signal in the mouse's abdominal cavity is weakened to a certain extent under a certain metabolic effect. It showed that the **Probe** can track SO_2 directly in vivo.

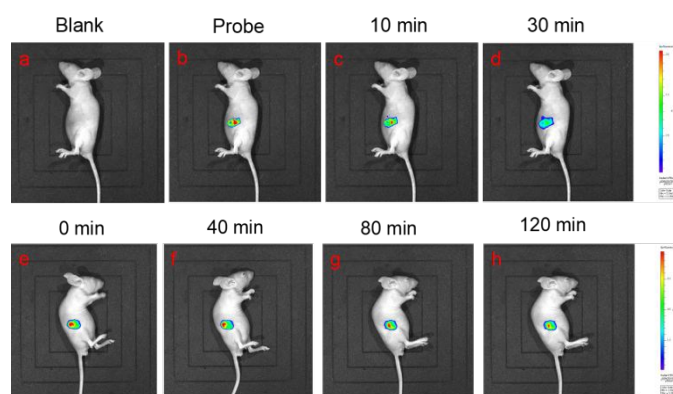


Figure 7. (a) Blank shooting. (b-d) After 10 min of NaHSO_3 (200 μM) injection, the **Probe** (20 μM) was injected, and then live fluorescence images at 0, 10, and 30 min. (e-h) After injecting, the real-time fluorescence image of the **Probe** at 0, 40, 80 and 120 min. $\lambda_{\text{ex}}=405\text{ nm}$, $\lambda_{\text{em}}=500\text{-}590\text{ nm}$.

3. Conclusion

In summary, we have designed and developed a ratiometric **Probe** based on the quinoline ring large conjugated architecture, which exhibited an Stokes shift of 170 nm, and had rapid response capability and low detection limit in aqueous phase. In biological imaging experiments, the **Probe** can be well accumulated in the mitochondria and successfully carry out internal and external experiments and mouse imaging.

Conflicts of interest

There are no conflicts to declare.

Acknowledgments

We thank the National Natural Science Foundation of China (No. 21775096, 21907062, 21878180), One hundred people plan of Shanxi Province, Shanxi Province "1331 project" key innovation team construction plan cultivation team (2018-CT-1), 2018 Xiangyuan County Solid Waste Comprehensive Utilization Science and Technology Project (2018XYSJDS-05), Shanxi Province Foundation for Returness (2017-026), Shanxi Collaborative Innovation Center of High Value-added Utilization of Coal-related Wastes (2015-10-B3), the Shanxi Province Foundation for Selected (No. 2019), Innovative Talents of Higher Education Institutions of Shanxi, Scientific and Technological Innovation Programs of Higher Education Institutions in Shanxi (2019L0031), Key R&D Program of Shanxi Province (201903D421069), the Shanxi Province Science Foundation (No. 201901D111015), Key R&D and transformation plan of Qinghai Province (No. 2020-GX-101 and Scientific Instrument Center of Shanxi University (201512).

References

- J.C. Xu, H.Q. Yuan, L.T. Zeng and G.M. Bao, *Chin. Chem. Lett.*, 2018, **29**, 1456-1464.
- Y.Y. Ma, Y.H. Tang, Y.P. Zhao and W.Y. Lin, *Anal. Chem.*, 2019, **91**, 10723-10730.
- Y.K. Yue, F.J. Huo, P. Ning, Y.B. Zhang, J.B. Chao, X.M. Meng and C.X. Yin, *J. Am. Chem. Soc.*, 2017, **139**, 3181-3185.
- L. Zhang, X.A. Liu, K.D. Gillis and T.E. Glass, *Angew. Chem. Int. Ed.*, 2019, **58**, 7611-7614.
- H.F. Jin, Y. Wang, X.B. Wang, Y. Sun, C.S. Tang and J.B. Du, *Nitric Oxide*, 2013, **32**, 56-61.
- S.X. Du, H.F. Jin, D.F. Bu, X. Zhao, B. Geng and C.S. Tang, *Acta Pharmacol. Sin.*, 2008, **29**, 923-930.
- L. Luo, S. Chen, H. Jin, C. Chang and J. Du, *Biochem. Bioph. Res. Co.*, 2011, **415**, 61-67.
- X. Y. Han, X.Y. Song, F.B. Yu and L.X. Chen, *Chem. Sci.*, 2017, **8**, 6991-7002.
- J. R. Stone and S. Yang, *Antioxid. Redox. Signal.*, 2006, **8**, 243-270.
- J.W. Lee and J.D. Helmann, *Nature*, 2006, **440**, 363-367.
- F.Y. Qin, Y.R. Zhang, J.M. Zhu, Y. Li, W.B. Cao and Y. Ye, *Sens. Actuators B Chem.*, 2019, **291**, 207-215.
- M.Y. Li, P.C. Cui, K. Li, J.H. Feng, M.M. Zou and X.Q. Yu, *Chin. Chem. Lett.*, 2015, **29**, 992-994.
- Y. Zhou, F.W. Zeng, Y. Liu, M. Li, S.Z. Xiao, J.Y. Yan, N.N. Zhang and K.B. Zheng, *Tetrahedron Lett.*, 2018, **59**, 3253-3257.

Journal Name

COMMUNICATION

- 14 F.H. Chen, A.K. Liu, R.X. Ji, Z.Y. Xu, J. Dong and Y.Q. Ge, *Dye Pigm.*, 2019, **165**, 212-216.
- 15 K.Y. Bi, R.Tan, R.T. Hao, L.X. Miao, Y.Q.He, X.H. Wu, J.F. Zhang and R. Xu, *Chin. Chem. Lett.*, 2019, **30**, 545-548.
- 16 X.G. Yang, Y.B. Zhou, X.F. Zhang, S. Yang, Y. Chen, J.R. Guo, X.X. Li, Z.H. Qing and R.H. Yang, *Chem. Commun.*, 2016, **52**, 10289-10292.
- 17 Y. Zhao, Y. Ma and W. Lin, *Sens. Actuators B Chem.*, 2018, **268**, 157-163.
- 18 Y. Ma, Y. Tang, Y. Zhao, S. Gao and W. Lin, *Anal. Chem.*, 2017, **89**, 9388-9393.
- 19 D. Li, Z. Wang, H. Su, J. Miao and B. Zhao, *Chem. Commun.*, 2017, **53**, 577-580.
- 20 K. Dou, G. Chen, F. Yu, Z. Sun, G. Li, X. Zhao, L. Chen and J. You, *J. Mater. Chem. B Mater. Biol. Med.*, 2017, **5**, 8389-8398.
- 21 H. Wang, D.L. Shi, J. Li, H.Y. Tang, J. Li and Y. Guo, *Sens. Actuators B Chem.*, 2018, **256**, 600-608.
- 22 M.J. Peng, X.F. Yang, B. Yin, Y. Guo, F. Suzenet, D. En, J. Li, C.W. Li, and Y.W. Duan, *Chem. Asian. J.*, 2014, **9**, 1817-1822.
- 23 Q.M. Liu, A.Y. Li, X.K. Li, B.L., Y.H. Zhang, J. Li and Y. Guo, *Sens. Actuators B Chem.*, 2019, **283**, 820-830.
- 24 Y. Guo, J. An, H.Y. Tang, M.J. Peng and F. Suzenet, *Mater. Res. Bull.*, 2015, **63**, 155-163.
- 25 J. Yang, K. Li, J.-T. Hou, C.-Y. Lu, L.-L. Li, K.-K. Yu, et al., *Sci. China Chem.*, 2017, **60**, 793-798.
- 26 K. Dou, Q. Fu, G. Chen, F. Yu, Y. Liu, Z. Cao, et al., *Biomaterials*, 2017, **133**, 82-93.
- 27 S. Chen, P. Hou, J. Wang and X. Song, *RSC Adv.*, 2012, **2**, 10869-10873.
- 28 S. Samanta, P. Dey, R. Aiyagari and G. Das, *Chem. Commun.*, 2016, **52**, 10381-10384.
- 29 Z. Liu, S. Guo, J. Piao, X. Zhou and X. Wu, *RSC Adv.*, 2014, **4**, 54554-54557.
- 30 J.L. Han, X.X. Yue, J.P. Wang, Y. Zhang, B.H. Wang and X.X. Song, *Chin. Chem. Lett.*, 2020, **31**, 1508-1510.
- 31 Y.Q. Sun, J. Liu, J. Zhang, T. Yang and W. Guo, *Chem. Commun.*, 2013, **49**, 2637-2639.
- 32 Q. Sun, W. Zhang and J. Qian, *Talanta*, 2017, **162**, 107-113
- 33 D. Wu, A.C. Sedgwick, T. Gunnlaugsson, E.U. Akkaya, J. Yoon and T.D. James, *Chem. Soc. Rev.*, 2017, **46**, 7105-7123.
- 34 K. Kikuchi, *Chem. Soc. Rev.*, 2010, **39**, 2048-2053.
- 35 T. Ma, F.J. Huo, J.B. Chao, J.G. Li and C.X. Yin, *Sens. Actuators B Chem.*, 2020, **320**, 128044.
- 36 T. Ma, F. J. Huo, Y. Wen, T. E. Glass and C. X. Yin, *Spectrochim. Acta, Part A*, 2019, **214**, 355-359.
- 37 Y.F. Huang, Y.B. Zhang, F.J. Huo, J.B. Chao, C.X. Yin, *Sens. Actuators B Chem.*, 2019, **287**, 453-458.

View Article Online
DOI: 10.1039/D0NJ04484A